NASA CONTRACTOR REPORT

NASA CR-112296

NASA CR-112296

FINITE ELEMENT APPROACH TO THE INTEGRATED POTENTIAL FORMULATION OF GENERAL UNSTEADY SUPERSONIC AERODYNAMICS

by Kari Appa and G. C. C. Smith

Prepared by

Bell Aerospace DIVISION OF textron
POST OFFICE BOX ONE
BUFFALO, NEW YORK 14240

for Langley Research Center

NATIONAL AERONAUTICS AND SPACE ADMINISTRATION • WASHINGTON, D. C.

NASA CR-112296

FINITE ELEMENT APPROACH TO THE INTEGRATED POTENTIAL FORMULATION OF GENERAL UNSTEADY SUPERSONIC AERODYNAMICS

By

Kari Appa and G.C.C. Smith

Prepared Under Contract No. NAS1-10880
Bell Aerospace Company
Buffalo, N.Y. 14240

for

NATIONAL AERONAUTICS AND SPACE ADMINISTRATION

CONTENTS

	Page
SUMMARY	1
INTRODUCTION	4
Mathematical Approach	5
Discretization	7
SYMBOLS	2
INTEGRAL EQUATION FORMULATION	8
COMPUTATIONAL METHOD	12
General Formulation	12
Influence of the Wake	21
Singular Integrals	22
DISCUSSION	26
APPENDIX	28
REFERENCES	33, 34

ILLUSTRATIONS

Figure		Page
1	Supersonic Flow Envelope About the Surface S	10
2	Integration Limits of a Complete Triangular Element	20
3	Integration Limits of a Partial Triangular Element	20
4	Wake Element in the Integrated Potential Method	23
A1	Local Coordinates and Components of Direction Cosines of a Typical Element	29
A2		32

TABLES

Number		
1	Comparison of Generalized Aerodynamic Forces for Rectangular Wing of Aspect Ratio 2.0 at $M_o = 1.2$	27

FINITE ELEMENT APPROACH TO THE INTEGRATED POTENTIAL FORMULATION OF GENERAL UNSTEADY SUPERSONIC AERODYNAMICS

by

Kari Appa*
and
G.C.C. Smith+

Bell Aerospace Company
Division of Textron Inc.

SUMMARY

Analytical formulation of the integrated potential approach for general unsteady supersonic configurations is related to numerical solution approaches using an arbitrary finite element mesh. Work remains to be done on adequate numerical handling of singular integrals, discussed in an appendix.

Limited results on a planar rectangular wing are presented.

---

* Chief, Dynamic Analysis

+ Chief Engineer, Structural Dynamics.

SYMBOLS

a_o	Speed of sound in free stream
$A_{11}, A_{12}, A_{21}, A_{22}$	Influence coefficient matrices in Eqn. 47
C	Defined by Equation 41a
f1, f2, f3 F_1, F_2, F_3, F_4	Functions defined by Equations 33 through 39
F	A typical function
G, G_s	Defined by Equations 53 and 56 respectively
J_{2r}	Bessel functions of order 2r
I_s	Singular integral
$\mathcal{L}$, L, L_o	Defined by Equations 19, 21 and 22.
ℓ_r	A reference length
M_o	Mach Number
r	Radius of a characteristic cone
R	Hyperbolic radius
S	Body Surface
t	Time
T	Transformation Matrix (Equation 30)
u_i	Velocity components in the ith coordinate direction
w	Normal wash
U	Flight Speed
V	Enclosed volume between leading Mach envelope and the characteristic surface
x_1, y_1, z_1	System Coordinates
X, Y, Z	Nondimensional transformed coordinates

SYMBOLS (CONT)

$X \equiv (X,Y,Z)$	A position vector
β	$(M_o^2 - 1)^{\frac{1}{2}}$
Γ	Characteristic Envelope
Γ_L	Leading Mach envelope
η	Deformation of body surface S
θ	Defined in Equation 9
k	$\frac{\lambda M_o}{\beta}$
$\lambda = \frac{\omega \ell_r}{U}$	Reduced frequency
γ, μ	Defined by Equations 25 and 26 respectively
ϕ, φ	Velocity potential (Equation 2)
Φ	A column vector of velocity potential at the corners of an element
ψ	Particular solution of Equation 3
ψ	Defined by Equation 25
ω	Circular frequency
Ω	Interpolation function (Equation 27 and 28)

Subscripts and Notations

o	Receiving field point
L, U	Lower and upper limits
$\frac{D}{Dt}( )$	Material derivative of the deformation of the body surface
$\frac{\partial}{\partial \eta}( )$	Normal derivative operator
$\frac{\partial}{\partial \nu}( )$	Co-normal derivative operator
Δ	Difference between two values.

INTRODUCTION

General. - Developments reported in References 1 and 2 have demonstrated the approach to unsteady supersonic aerodynamic determinations based on matrix/consistent element formulations. "Consistent aerodynamic element" implies a transition from real continuous variables (downwash, displacement, potential, etc.) to numerical discrete variables, such that variationally equivalent work is done. Additionally, the arbitrary shape and orientation of the (triangular) element enables effective matching of problem boundaries. These two features were contrasted with general Mach box approaches in References 3 - 7.

For shuttle-type flight vehicles with comparatively large body diameter to wing span ratio, non-linear body interference on the lifting surfaces is very significant in determining the unsteady forces involved in flutter. In steady flow, thickness may be taken into account in an approximate fashion by a "local linearization" and replacement of the nonlinear equations by locally linear ones with variable coefficients. Mathematical justification is discussed in References 8 and 9. In the case of unsteady flow this approach suggests that the fluid motion might be calculated with satisfactory accuracy from linearized, unsteady equations containing local values of the flow parameters as affected by thickness, mean surface gradient, etc. (References 10, 11, 12.)

Additionally the downwash/potential integration formulation in Reference 2 has disadvantages when considered for use in more complex configurations, and other approaches to the integral formulation should be considered.

The present task was to formulate an extension of the consistent element approach involving two steps:

a) a change from a downwash/potential formulation to an "integrated potential" formulation (Ref. 13)

b) the incorporation of arbitrary element attitude to encompass more general configurations and space-variable flows.

This report outlines initial developments for such problems including

(1) choice and evolution of an acceptable analytical approach;

(2) construction of "consistent finite element" idealization compatible with structural aspects of the problem;

(3) data handling and computational procedures at a pilot program level;

(4) discussion of future generalization.

It was assumed that some "best" method of defining the steady field exists as a basis for superposing the linearized unsteady perturbation (e.g. Ref. 14).

Mathematical Approach

Due to the complexity of the linear integral equation kernels relating downwash and velocity potential or pressure, general analytical solutions for arbitrary Mach numbers, planforms, and frequency parameters are not available. Consequently, several numerical approaches, with various advantages and disadvantages, have been developed. The three most frequently employed methods are:

1. The Collocation Method. - This method uses the integral relation between the downwash at a point and the loading/acceleration potential assumed on the lifting surface lying in its forward-Mach cone region, (e.g. Ref. 15). The simplicity of this method is that it yields directly the loading corresponding to any given downwash vector. However, a severe short-coming of the method is that discontinuous loading requires special choice of the loading functions. Also, for high frequency parameters, the loading functions become highly oscillatory, requiring very close collocation points in the chordwise and spanwise directions.

2. The Integrated Downwash Method. - This method yields velocity potential at any point as an integral relation between downwash and source, dipole or quadrupole distributions in the forward Mach cone region (Refs. 1 to 7, 16, 17). In the case of subsonic leading edges or in "interference" cases, downwash or source strengths in the so-called 'diaphragm surfaces' are unknown and must be determined from the condition of zero diaphragm pressure difference. However, at low supersonic Mach numbers the diaphragms may be much larger than the lifting surface and the approach becomes very inefficient from computational time and storage points of view. Another serious drawback of this method lies in difficulties of determining the downwash/source strengths along singular leading edges.

   For problems with interference the method requires both source-downwash and potential-source strength solutions adding to the total computational effort needed.

3. The Integrated Potential Method. - (Refs. 13, 18, 19) This method yields the velocity potential at a point as an integral involving the velocity potential taken over the forward Mach Cone region. Since the potential difference across diaphragms is zero, consideration of these regions is not required.

   The advantages of this method are:

   1. diaphragm regions are avoided; therefore problems involving determination of singular downwash terms/source strengths in wakes are eliminated;

2. velocity potentials can be more easily approximated, since they are continuous;
3. it should be computationally efficient compared with method 2, especially for complex configurations.

Discretization

For thick bodies in supersonic flow, local velocity and Mach number distribution vary considerably. Any numerical method using characteristic grid systems requires change of the grid system with local Mach number. In the present approach, "consistent finite element" formulations are used in a fixed grid system which can account approximately for small variations of local mean flow parameters; e.g., local Mach number and velocity vector due to non-slender configuration.

The basic advantages of the finite element integrated potential formulation are formidable.

1. Excellent boundary representations of leading, trailing and tip edges of wings, etc., compared with box and "sub-box" representations;
2. Possibility of tailoring other elements to nacelle and body representations (e.g., ring and conical "shell" elements);
3. Flexibility with respect to element type, size, and orientation so that grid point density can be varied compatible with spatial loading variations;
4. Kinematically consistent downwash, loading and generalized force derivations;
5. Efficient handling of wake interference in that wake edges can in effect, constitute a "single element";

6. Feasibility of using common structural-aerodynamic grids is convenient for optimization problems;

7. Formulation for locally varying Mach number is possible, given a steady state flow field distribution.

These advantages are expected to be even stronger in more complex geometries such as wing-body interaction in terms of feasibility of adequate modelling and economy of computational effort.

INTEGRAL EQUATION FORMULATION

The following development parallels that of Ref. 13 to a large extent, the basic differences being (i) the extension of the formulation from planar surfaces to arbitrary bodies (within the bounds of a linearizable approach), and (ii) the retention of the local Mach number parameter β so that some approximate handling of its effect in a variable Mach number field is facilitated.

The velocity potential ϕ (such that $\frac{\partial \phi}{\partial x_i} = u_i$) satisfies

$$\frac{\partial^2 \phi}{\partial t^2} + 2V \frac{\partial^2 \phi}{\partial x_1 \partial t} + V^2 \frac{\partial^2 \phi}{\partial x_1^2} = a_o^2 \nabla^2 \phi \tag{1}$$

which transforms, using

$$\phi = \varphi \exp\left(-\frac{i\lambda M_o^2 X}{\beta}\right) \exp(i\lambda T) \tag{2}$$

to

$$\frac{\partial^2 \varphi}{\partial Y^2} - \frac{\partial^2 \varphi}{\partial Z^2} - \frac{\partial^2 \varphi}{\partial X^2} - k^2 \varphi \equiv L(\varphi) = 0 \tag{3}$$

in which $X = x_1/\beta \ell_r$, $Y = y_1/\ell_r$, $Z = z_1/\ell_r$ are the non-dimensional coordinates with respect to the reference length ℓ_r

Defining $X_o = (X_o, Y_o, Z_o)$ a field point, and

$$x = (X_o - X),\ y = (Y_o - Y),\ z = (Z_o - Z),$$

the characteristic cone from X_o is the surface

$$x^2 - y^2 - z^2 \equiv x^2 - r^2 = 0 \tag{4}$$

If ψ is some particular solution of (3), the generalized Green's theorem states

$$\int_V \left[\psi L(\varphi) - \varphi L(\psi)\right] dV = \int_S \left[\varphi \frac{\partial \psi}{\partial \nu} - \psi \frac{\partial \varphi}{\partial \nu}\right] dS \tag{5}$$

In equation (5) $\frac{\partial}{\partial \nu} = -\ell \frac{\partial}{\partial X} + m \frac{\partial}{\partial Y} + n \frac{\partial}{\partial Z}$

is a differential operator, ν is the co-normal such that ℓ, m, n are direction cosines of the normal on S into V. (Fig. 1) S and V are taken as the surface and volume defined by Γ_1 the leading wave front, Γ_2 the forward characteristic surface from X_o, and the body surface. Since L (φ) = L (ψ) = 0, Equation (5) becomes

$$\int_S \left[\varphi \frac{\partial \psi}{\partial \nu} - \psi \frac{\partial \varphi}{\partial \nu}\right] dS = 0 \tag{6}$$

On the wavefront Γ_1, φ and $\frac{\partial \varphi}{\partial \nu} = 0$, hence if ψ is chosen such that ψ and $\frac{\partial \psi}{\partial \nu}$ are zero on Γ, Eqn (6) becomes

$$\int_{\text{Body}} \left(\varphi \frac{\partial \psi}{\partial \nu} - \psi \frac{\partial \varphi}{\partial \nu}\right) dS = 0 \tag{7}$$

Ref. 13 gives the appropriate ψ's as

$$\left.\begin{aligned} \psi_1 &= \frac{\sin q}{q} \log_e (\theta + \sqrt{\theta^2 - 1}) \\ \psi_2 &= -\frac{x}{q}\left[\frac{\partial}{\partial q}\left(\frac{\sin q}{q}\right)\right]\left[\log_e\left[\theta + \sqrt{\theta^2 - 1}\right] - \frac{\sqrt{\theta^2 - 1}}{\theta}\right] \end{aligned}\right\} \tag{8}$$

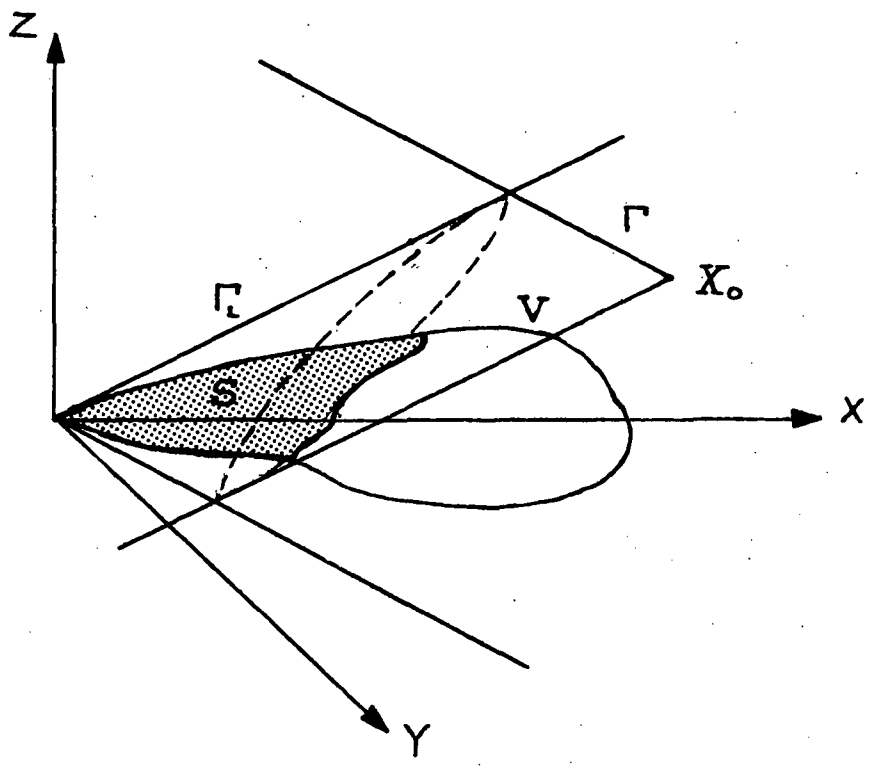

Figure 1 Supersonic Flow Envelope About The Surface S

(which are singular on $x = r$), and where

$$q^2 = k^2(x^2 - r^2) \quad , \quad \theta = \frac{x}{r} \tag{9}$$

By the common potential theory maneuver of excluding the singularities by small limiting surfaces and proceeding to a limit, Eq. (7) becomes

$$\varphi(X_o) = \frac{1}{2\pi}\int_S \left[\varphi(X)\,\frac{\partial}{\partial \nu}\left(\frac{\cos kR}{R}\right) - \left(\frac{\cos kR}{R}\right)\frac{\partial \varphi}{\partial \nu}\right] dS \tag{10}$$

where

$$R^2 = x^2 - r^2 \tag{11}$$

Using Eq. (2), and dropping $\exp(i\lambda T)$ throughout

$$\phi(X_o) = \frac{1}{2\pi}\iint\left[\left\{\frac{\partial}{\partial \nu}\left(\frac{\cos kR}{R}\right) + ik\ell M_o\left(\frac{\cos kR}{R}\right)\right\}\phi(X) - \left(\frac{\cos kR}{R}\right)\frac{\partial \phi}{\partial \nu}\right]\exp\left(-ikM_o(X_o - X)\right) dS \tag{12}$$

Defining the "normal" derivative at a field point X_o

$$\frac{\partial}{\partial \eta_{1_o}} = \ell_{1_o}\frac{\partial}{\partial x_{1_o}} + m_{1_o}\frac{\partial}{\partial y_{1_o}} + n_{1_o}\frac{\partial}{\partial z_{1_o}} = \frac{1}{\ell_r}\frac{\partial}{\partial \eta_o} \tag{13}$$

the normal velocity at this point is

$$w = \frac{\partial \phi(X_o)}{\partial \eta_{1_o}} = \frac{1}{\ell_r}\frac{\partial \phi(X_o)}{\partial \eta_o} \tag{14}$$

Then,

$$\frac{\partial \phi(X_o)}{\partial \eta_{1_o}} = \frac{1}{2\pi\ell_r}\iint \frac{\partial}{\partial \eta_o}\left[\exp\left(ikM_o(X_o - X)\right)\left\{\frac{\partial}{\partial \nu}\left(\frac{\cos kR}{R}\right) + ikM_o\ell\,\frac{\cos kR}{R}\right\}\phi(X) - \frac{\cos kR}{R}\,\frac{\partial \phi}{\partial \nu}(X)\right] dS \tag{15}$$

$$\text{or}\quad \frac{\partial \phi(X_o)}{\partial \eta_{1_o}} = \frac{1}{2\pi \ell_r}\int \exp\left(-ikM_o(X_o - X)\right)\Bigg[\left\{\frac{\partial^2}{\partial \eta_o \partial \nu}\left(\frac{\cos kR}{R}\right) + k^2 M_o^2 \ell_{1_o}\ell \frac{\cos kR}{R} + ikM_o\left\{\ell \frac{\partial}{\partial \eta_o}\left(\frac{\cos kR}{R}\right) - \ell_{1_o}\frac{\partial}{\partial \nu}\left(\frac{\cos kR}{R}\right)\right\}\right\}\phi(X)$$

$$-\left\{\frac{\partial}{\partial \eta_o}\left(\frac{\cos kR}{R}\right) - ikM_o \ell_{1_o}\frac{\cos kR}{R}\right\}\frac{\partial \phi}{\partial \nu}(X)\Bigg]\, dS \qquad (16)$$

For panels on thin wings and on bodies (i.e., with flow on both sides and one side respectively) handling of the $\Delta\phi$ (difference) and $\Delta\frac{\partial\phi}{\partial\nu}$ requires some comment, condensed in the following:

	$\Delta\phi$	$\Delta\frac{\partial\phi}{\partial\nu}$
Panel of a thin surface	Nonzero if interference occurs	Nonzero in interfering case Zero for non-interfering case.
Panel of a body	Nonzero	Nonzero in general

Allen & Sadler, (Ref. 20), Woodcock (Refs. 18, 21) consider $\partial\phi/\partial\nu$ to be identically zero for plate-like elements. However, $\Delta\partial\phi/\partial\nu$ is not zero for interfering cones such as will occur in wing-body interference. This term can and will be considered in future developments in this work.

COMPUTATIONAL METHOD

General Formulation

The integral equations (12&16) for the potential are so complex that closed form solutions are not considered. Numerical integration methods are invariably employed for which Refs. 20 & 21 for example, use characteristic grid systems. In these analyses,

non-singular terms within each element are expressed by means of interpolation functions while singular terms are evaluated considering only the finite part of the integrals. For planar elements, the singular terms are few in number and the singular integrations may not affect the results significantly. However, in non-planar cases the integrals in Equation (16) are strongly singular and there are more terms than in planar cases. This section discusses the possible means of reducing the number of singular terms, and the extent or domain of singular functions.

The kernel $\left(\frac{\cos kR}{R}\right)$ in Equation (16) exhibits square root singularity as the characteristic surface is approached. This form of singularity can be expressed by a well-behaved Bessel series Refs. (3) and (22). Performing the required normal derivation and simplifying the terms, the velocity potential and downwash integrals can be written as

$$\varphi(X_o) = -\frac{1}{2\pi}\iint \exp\left\{-ikM_o\Delta X\right\}\left[\left\{\frac{L(X)}{\Delta X}\cdot\frac{\partial}{\partial X}\left(\frac{\partial\psi}{\partial Y}\right) - ikM_o\ell\frac{\partial\psi}{\partial Y}\right\}\Phi - \frac{\partial\psi}{\partial Y}\frac{\partial\Phi}{\partial\vec{\nu}}\right]dS \tag{17}$$

and the downwash integral as

$$\frac{\partial\phi(X_o)}{\partial\vec{n}_o} = -\frac{1}{2\pi\ell_r}\iint \exp\left\{-ikM_o\Delta X\right\}\left[\left\{\frac{\mathcal{L}(X)}{\Delta X}\frac{\partial}{\partial X}\left(\frac{\partial\psi}{\partial Y}\right) + k^2\left(M_o^2\ell_o\ell - \frac{L_o(X)L(X)}{R^2}\right)\frac{\partial\psi}{\partial Y}\right\}\Phi - \left\{\frac{L_o(X)}{\Delta X}\frac{\partial}{\partial X}\left(\frac{\partial\psi}{\partial Y}\right) + ikM_o\ell_o\frac{\partial\psi}{\partial Y}\right\}\frac{\partial\Phi}{\partial\vec{\nu}}\right]dS \tag{18}$$

In these equations,

$$\mathcal{L}(X) = \left[- \overline{LL}_o + \frac{3 L_o(X) L(X)}{R^2} + ikM_o \left\{ \ell_o L(X) - \ell L_o(X) \right\} \right] \quad (19)$$

in which $\overline{LL}_o = (\ell_o \ell + m_o m + n_o n)$ (20)

$$L(X) = -\ell \Delta X + m \Delta Y + n \Delta Z \quad (21)$$

$$L_o(X) = \ell_o \Delta X + m_o \Delta Y + n_o \Delta Z \quad (22)$$

and $\Delta X = (X_o - X)$, $\Delta Y = (Y_o - Y)$, $\Delta Z = (Z_o - Z)$

Watson's relation (Ref. 22), is

$$\frac{\cos kR}{R} = - \frac{\partial \psi}{\partial Y} \quad (23)$$

in which

$$\psi(\mu, \gamma) = J_o(k\mu) \sin^{-1}\left(\frac{\gamma}{\mu}\right) + \sum_r \frac{(-1)^r J_{2r}(k\mu)}{r} \sin\left(2r \sin^{-1}\left(\frac{\gamma}{\mu}\right)\right) \quad (24)$$

with $\gamma = Y_o - Y$ (25)

and $\mu = \sqrt{(X_o - X)^2 - (Z_o - Z)^2}$ (26)

The velocity potential in Equation (17) is singular only at the apex of the characteristic cone, while the normal wash integral has singular terms at the apex and on the characteristic surface for a general configuration. However, for a planar case the singularity in the normal wash term is limited to the apex only.

The numerical integrations of Equations (17) and (18) can be performed on any convenient discrete element basis such as triangular, quadrilateral or conical ring elements. This idealization requires description of the doublet ($\Delta\varphi$) or source ($\Delta \partial\varphi/\partial\vec{v}$) distributions within each element in terms of its nodal or boundary values. These distributions might be limited to linear or quadratic expressions in space coordinates.

Triangular Element. - These are the simplest elements suitable for many irregular configurations. Curved surfaces can be represented adequately with a sufficient number of flat triangles.

Quadrilateral Element. - Consideration of quadrilateral elements in place of triangular elements is valuable in terms of computational efficiency for a given flat lifting surface.

Conical Ring Element. - For axisymmetric bodies of revolution it is possible to use a circumferential description of normal wash and the corresponding doublet/source distributions in the form of Fourier sine or cosine series.

To demonstrate the method consider the triangular element with a linear distribution of doublet or source strength, i.e.,

$$\Delta\phi = \Omega(X,Y)\,\Delta\Phi \tag{27}$$

or

$$\Delta\frac{\partial\phi}{\partial\vec{\nu}} = \Omega(X,Y)\,\Delta\frac{\partial\Phi}{\partial\vec{\nu}} \tag{28}$$

where $\Omega(X,Y) = [\,X \;\; Y \;\; 1\,]\,T$ is a transformation matrix, (29)

in which

$$T = \begin{bmatrix} X_1 & Y_1 & 1 \\ X_2 & Y_2 & 1 \\ X_3 & Y_3 & 1 \end{bmatrix}^{-1} \tag{30}$$

and $\Delta\phi$ and $\Delta\,\partial\phi/\partial\vec{\nu}$ are the values of the source and doublet strengths respectively at the vertices of the triangle. Using (27) and (28) in Equations (17) and (18), the velocity potential and normal wash integrals for each element in the domain of influence are given by:

$$\Delta\phi(X_0) = -\frac{c}{2\pi}\iint \exp(-ikM_0\Delta X)\left[\left\{\frac{f_1}{\Delta X}\frac{\partial}{\partial X}\left(\frac{\partial\psi}{\partial Y}\right) - f_2\frac{\partial\psi}{\partial Y}\right\}\Delta\Phi - \left\{f_3\frac{\partial\psi}{\partial Y}\right\}\Delta\frac{\partial\Phi}{\partial\vec{v}}\right]dS \qquad (31)$$

and

$$w = \frac{c}{2\pi\ell_r}\iint \exp\left\{-ikM_0\Delta X\right\}\left[\left\{\frac{F_1}{\Delta X}\frac{\partial}{\partial X}\left(\frac{\partial\psi}{\partial Y}\right) + F_2\frac{\partial\psi}{\partial Y}\right\}\Delta\Phi - \left\{\frac{F_3}{\Delta X}\frac{\partial}{\partial X}\left(\frac{\partial\psi}{\partial Y}\right) + F_4\frac{\partial\psi}{\partial Y}\right\}\Delta\frac{\partial\Phi}{\partial\vec{v}}\right]dS \qquad (32)$$

respectively.

The following definitions are observed in equations (31) and (32);

$$f_1 = L(X)\,\Omega(X,Y) \qquad (33)$$

$$f_2 = ikM_0\ell\,\Omega(X,Y) \qquad (34)$$

$$f_3 = \Omega(X,Y) \qquad (35)$$

$$F_1 = \mathcal{L}(X)\,\Omega(X,Y) \qquad (36)$$

$$F_2 = k^2\left(M_0^2\ell_0\ell - \frac{L_0(X)L(X)}{R^2}\right)\Omega(X,Y) \qquad (37)$$

$$F_3 = L_0(X)\,\Omega(X,Y) \qquad (38)$$

$$F_4 = ikM_0\ell_0\,\Omega(X,Y) \qquad (39)$$

The general forms of the integrals in Equations (31) and (32) are of only two types, i.e., involving single and cross-derivatives of the function ψ. The function ψ is well behaved

in the fore Mach Cone region, but its derivatives are non-analytic on the characteristic surface. The functions such as f_1 to f_3 and F_1 to F_4 (with the exception of the term $L_o(X)L(X)/R^2$ in F_1 and F_2 which will be discussed later under singular integrals) are also analytic throughout the domain of integration.

To take advantage of the well-conditioned function ψ, it is necessary to cast the integrands in a particular form for numerical integration. Consider for example an integral of the form

$$I = \iint \exp\{-ikM_o\Delta X\} \frac{F}{\Delta X} \frac{\partial}{\partial X}\left(\frac{\partial \psi}{\partial Y}\right) dS \tag{40}$$

in which the function F is analytic throughout the domain of dependence.

In performing numerical integration the infinitesimal surface area dS can be treated as that projected onto a plane whose unit normal is parallel to the normal of the element under consideration, e.g., if the normal of the element is close to the Z-axis then the infinitismal area

$$dS = \sqrt{1+\left(\frac{\partial Z}{\partial X}\right)^2+\left(\frac{\partial Z}{\partial Y}\right)^2}\; dX\,dY$$
$$= C(X,Y)\,dX\,dY \tag{41a}$$

On the other hand, if the unit normal is close to the Y axis, then

$$dS = \sqrt{1+\left(\frac{\partial Y}{\partial X}\right)^2+\left(\frac{\partial Y}{\partial Z}\right)^2}\; dX\,dZ \tag{41b}$$

Using (41a) the integral is

$$I = \int_{X_L}^{X_u} \frac{\exp\{-ikM_o\Delta X\}}{\Delta X} \int_{Y_L(X)}^{Y_u(X)} F \frac{\partial}{\partial X}\left(\frac{\partial \psi}{\partial Y}\right) dY\,dX \tag{42}$$

The integrand under the Y integral can be rewritten as

$$F\frac{\partial}{\partial X}\left(\frac{\partial \psi}{\partial Y}\right) = \frac{\partial}{\partial X}\left(\frac{\partial}{\partial Y}(F\psi)\right) - \frac{\partial}{\partial X}\left(\frac{\partial F}{\partial Y}\psi\right) - \frac{\partial}{\partial Y}\left(\frac{\partial F}{\partial X}\psi\right) + \frac{\partial^2 F}{\partial X\,\partial Y}\psi \tag{43}$$

Using Equation (43) in Equation (42), performing integration by parts, and using Leibnitz's rule for differentiation under the integral sign, the integral becomes

$$I_1 = \left[\frac{F_1(X_U, Y_U(X_U)).\psi(X_U, Y_U(X_U)) - F_1(X_U, Y_L(X_U)).\psi(X_U, Y_L(X_U))}{\Delta X}\right.$$

$$\left. - \frac{F_1(X_L, Y_U(X_L)).\psi(X_L, Y_U(X_L)) - F_1(X_L, Y_L(X_L)).\psi(X_L, Y_L(X_L))}{\Delta X}\right]$$

$$- \int_{X_L}^{X_U} \left[\frac{F_1(X, Y_U(X)).\psi(X, Y_U(X)) - F_1(X, Y_L(X)).\psi(X, Y_L(X)) + \Delta X\left\{\frac{\partial F_1(Y_U(X))}{\partial X}.\psi(Y_U(X))\right\}}{\Delta X^2}\right.$$

$$\left. - \frac{\Delta X\left\{\frac{\partial F_1(Y_L(X))}{\partial X}.\psi(Y_L(X) + \frac{\partial Y_U}{\partial X}.\frac{\partial F_1(X, Y_U(X))}{\partial Y}.\psi(X, Y_U(X)) - \frac{\partial Y_L}{\partial X}.\frac{\partial F_1(Y_L(X))}{\partial Y}.\psi(X, Y_L(X))\right\}}{\Delta X^2}\right] dX$$

$$- \left[\frac{1}{\Delta X_U}\int_{Y_L(X_U)}^{Y_U(X_U)} \frac{\partial F_1}{\partial Y}(X_U, Y).\psi(X_U, Y)\,dY - \frac{1}{\Delta X_L}\int_{Y_L(X_L)}^{Y_U(X_L)} \frac{\partial F_1}{\partial Y}(X_L, Y).\psi(X_L, Y)\,dY\right]$$

$$+ \int_{X_L}^{X_U}\left[\frac{1}{\Delta X^2}\left\{\int_{Y_L(X)}^{Y_U(X)} \frac{\partial F_1}{\partial Y}.\psi\,dY + \Delta X\int_{Y_L(X)}^{Y_U(X)} \frac{\partial^2 F_1}{\partial X\,\partial Y}.\psi\,dY\right\}\right] dX \qquad (44)$$

The first and the last terms vanish for elements with no sides parallel to the Y-axis. The numerical integration utilizes Gaussian weights and pivotal points. Limits of integration for complete and partial elements are shown in Figures 2 and 3.

The second set of integrals is the one with a single derivative of the function ψ i.e.,

$$I_2 = \int_{X_L}^{X_U} \exp\{-ikM_o\Delta X\} \int_{Y_L(X)}^{Y_U(X)} F(X,Y)\,\frac{\partial \psi}{\partial Y}\,dY\,dX \tag{45}$$

Performing partial integration, Equation (44) can be written as

$$I_2 = \int_{X_L}^{X_U} \left[\left\{ F(X,Y_U(X))\,\psi(X,Y_U(X)) - F(X,Y_L(X))\,\psi(X,Y_L(X)) \right\} - \int_{Y_L(X)}^{Y_U(X)} \frac{\partial F}{\partial Y}\,\psi\,dY \right] dX \tag{46}$$

Using the form of the integrals given by equations (44) and (46), the normal-wash integration in Equation (32) will be evaluated for all elements in the fore Mach Cone zone.

Considering all nodes on the lifting surface the velocity potential and normal wash in matrix notation are given by:

$$\Delta\Phi = A_{11}\,\Delta\frac{\partial\Phi}{\partial\vec{v}} + A_{12}\,\Delta\Phi$$

and

$$\frac{D\eta}{Dt} = A_{21}\,\Delta\frac{\partial\Phi}{\partial\vec{v}} + A_{22}\,\Delta\Phi \tag{47}$$

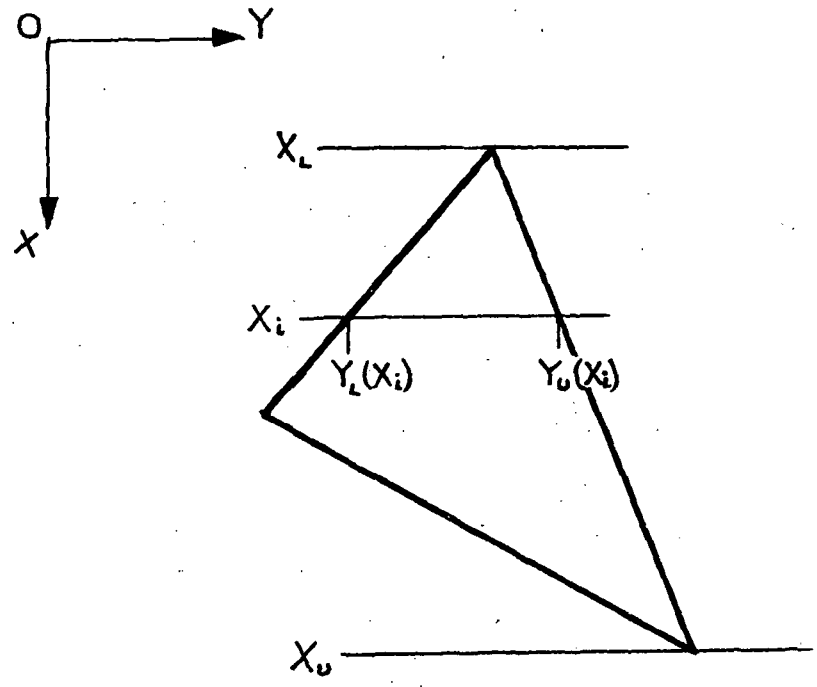

Figure 2 Integration Limits of A Complete Triangular Element

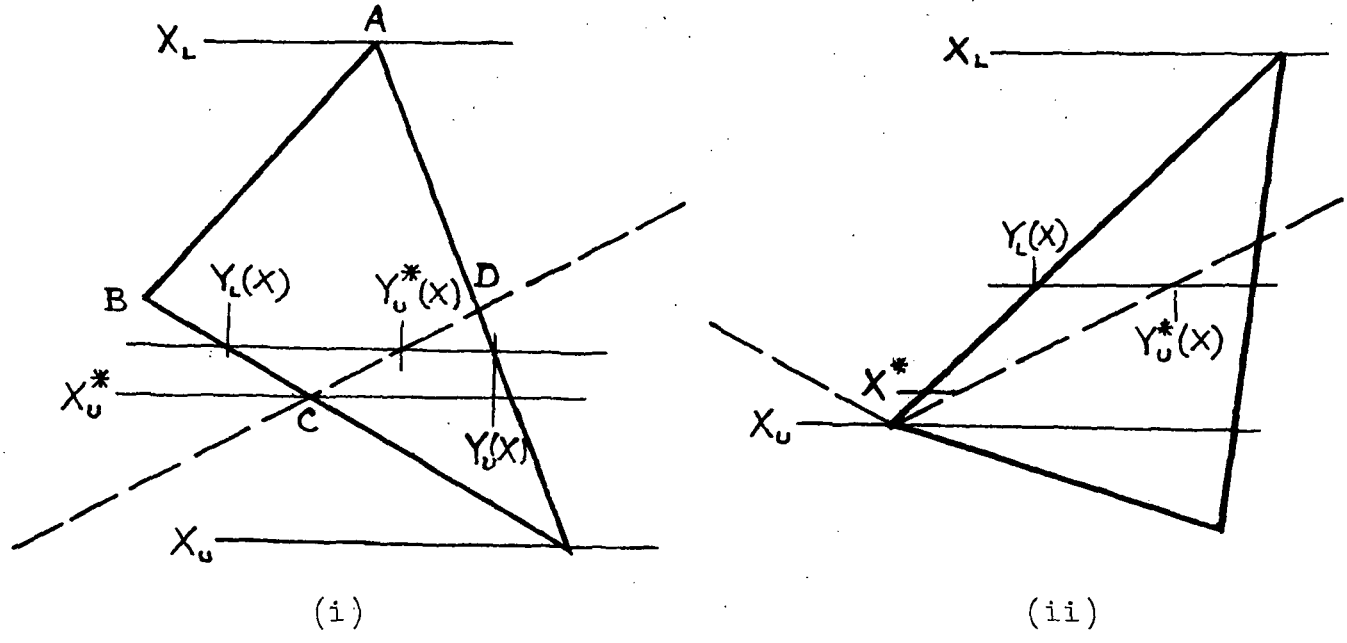

Figure 3 Integration Limits of a Partial Triangular Element

Woodcock and York (Ref. 21) consider $\Delta \partial\phi/\partial\vec{v} \Rightarrow 0$ for antisymmetric distribution of velocity potential on the upper and lower surfaces of a panel. However, in the presence of the interference, since $\phi_+ \neq \phi_-$, it appears that a differential source distribution is required to satisfy the normal wash condition in the second set of equations in (47). These two sets of distributions can be solved from the two sets of equations in (47). However, based on other analyses which omit these terms, (Ref. 21) the neglect of the term $\Delta \partial\phi/\partial\vec{v}$ is obviously sometimes justifiable. An independent study might be conducted to reveal its general significance.

Influence of the Wake

Determination of velocity potential for wings with subsonic trailing edges or tandem surfaces is very much influenced by velocity components in the wake region of the forward wing. It is a difficult task to determine the equilibrium position of a wake sheet even in the case of steady flow for a simple configuration. However, linearized computation methods assume that the wake sheet remains planar with the trailing edge (planes) panels. Having defined the assumed position of the wake sheet the velocity potential difference across the sheet can be evaluated in terms of the trailing edge values only. Since the pressure difference across the wake sheet is zero the potential difference is given by

$$\Delta\phi(X,Y) = \Delta\phi_{TE}(Y(X)) \exp\left\{-ik M_o \left(\frac{\beta^2}{M_o^2}\right)(X - X_{TE})\right\} \tag{48}$$

The potential in the wake is therefore dependent only on the trailing edge nodal values and there is no need to distribute elements in the wake region, (in contrast to the integrated downwash approach). Instead line elements of trailing edge can be used to describe the variation of $\Delta\phi_{TE}$. The integrals involved in the normal wash are essentially the same as in Equation (18),

with the following terms replaced, i.e.,

$$\exp\{-ikM_o\Delta X\} \quad \text{replaced by} \quad \exp\left\{-ikM_o\left(X_o-\left(1+\frac{\beta^2}{M_o^2}\right)X - \frac{\beta^2}{M_o^2}X_{TE}\right\}\right. \tag{49}$$

and

$$\Omega = [X \;\; Y \;\; 1]T \quad \text{replaced by} \quad \Omega_\omega = \begin{bmatrix} \frac{Y_u-Y}{Y_u-Y_L} & \frac{Y-Y_L}{Y_u-Y_L} \end{bmatrix} \tag{50}$$

The upper limits of X are determined from the vanishing of the hyperbolic radii of the characteristic envelope. (See Figure 4).

Singular Integrals

Equation (32) contains singular integrands as the integration limits approach the characteristic cone. Accuracy of solutions depends critically on numerical treatment of these singular functions. For this reason, the number of singular integrals involved has been reduced by certain transformations. Numerical computation of singular integrals is discussed in this section.

The general form of singular integrals is given by

$$I_s = \int_{X_L}^{X_u} \frac{\exp\{-ikM_o\Delta X\}}{\Delta X} \int_{Y_L(X)}^{Y_u(X)} F(X,Y)\,\frac{\partial}{\partial X}\left(\frac{\partial \psi}{\partial Y}\right) dY\,dX \tag{51}$$

where

$$F(X,Y) = \left[\mathcal{L}(X_o) + \frac{L_o(X)\,L(X)}{R^2}\right] \tag{52}$$

Let

$$G(X_i) = \int_{Y_L(X_i)}^{Y_u(X_i)} \left[\mathcal{L}(X) + \frac{L_o(X)\,L(X)}{R^2}\right] \frac{\partial}{\partial X}\left(\frac{\partial \psi}{\partial Y}\right) dY \tag{53}$$

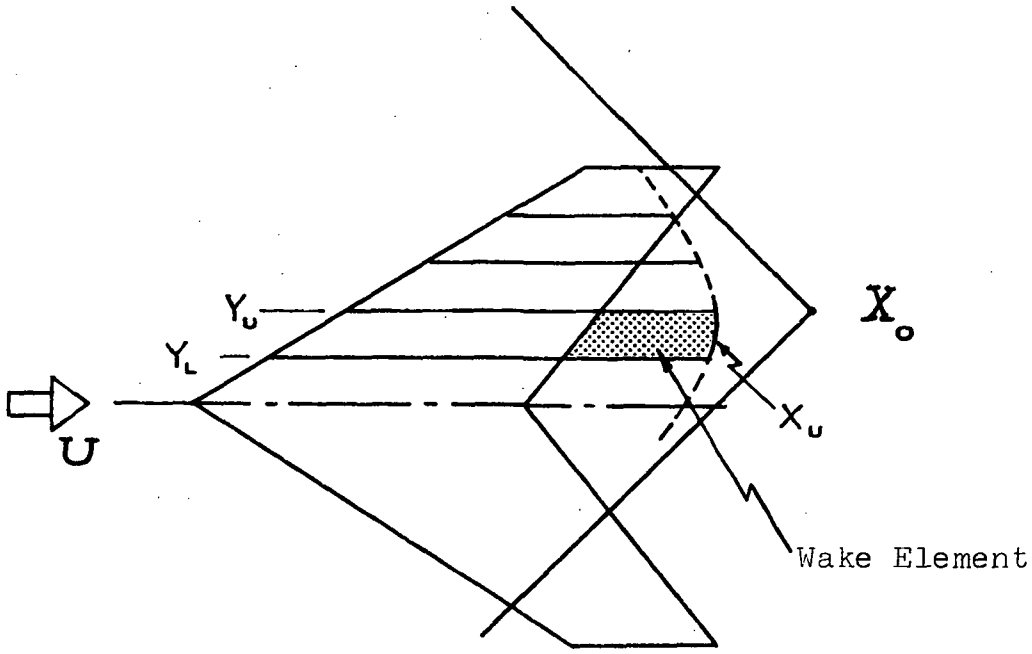

Figure 4 Wake Element In The Integrated Potential Method

The first term in Equation (53) is non-singular and hence can be integrated by parts. The second term is zero for coplanar elements, while for non-coplanar elements it becomes singular as the field point approaches the characteristic surface.

Figure (3) shows two forms of element interception by the Mach Cone, i.e.,

(i) when the element is away from the receiving point;
(ii) when the receiving point lies on a node of an element.

Case i

Put

$$G_s(X_i) = \int_{Y_L(X_i)}^{Y_U(X_i)} \frac{L_o(X)L(X)}{R^2} \frac{\partial}{\partial X}\left(\frac{\partial \psi}{\partial Y}\right) dY \tag{54}$$

where X_i is the ith Gaussian integration pivot in the X direction. Since the function ψ is well behaved over the area ABCD, Fig. 3, it can be expressed in terms of its nodal or boundary values, i.e.

$$\psi = \sum_{\substack{i=0,1,\cdots \\ j=0,1,\cdots}} a_{ij} X^i Y^j \tag{55}$$

Then performing the required differentiation, Equation (54) can be written as

$$G_s(X_i) = \int_{Y_L(X_i)}^{Y_U(X_i)} \frac{F(X,Y)\, dY}{R^2} \tag{56}$$

Let $Y^*(X_i)$ be the last Y coordinate in the Gaussian integration. Then Hadamard's finite part of the integral is given by

$$G_s(X_i) = \int_{Y_L(X_i)}^{Y_U(X_i)} \frac{(F(X_i,Y) - F(X_i,Y^*))}{R^2} dY + F(X_i,Y^*) \int_{Y_L(X_i)}^{Y_U(X_i)} \frac{dY}{R^2} \tag{57}$$

The last term in Equation (57) is given by

$$\int_{Y_L(X_i)}^{Y_U(X_i)} \frac{dY}{R^2} = -\frac{1}{2[\Delta X_i^2 - \Delta Z_i^2]^{1/2}} \left[\ln \left(\frac{(\Delta X^2 - \Delta Z^2)^{1/2} + \Delta Y}{(\Delta X^2 - \Delta Z^2)^{1/2} - \Delta Y} \right) \right]_{Y=Y_L}^{Y=Y_U}$$

$$(\text{for } \Delta X^2 - \Delta Z^2 \neq 0)$$

$$= \left[\frac{1}{\Delta Y} \right]_{Y_L}^{Y_U} \tag{58}$$

Considering only the finite part of Equation 58, the finite part of the singular integral Equation (57) is given by

$$G_s(X_i) = \int_{Y_L(X_i)}^{Y_U(X_i)} \frac{F(X_i,Y) - F(X_i,Y^*)}{R^2} dY - \frac{F(X_i,Y)}{2[\Delta X^2 - \Delta Z^2]^{1/2}} \ln \left[\frac{[\Delta X^2 - \Delta Z^2]^{1/2} - \Delta Y}{[\Delta X^2 - \Delta Z^2]^{1/2} + \Delta Y} \right]$$

$$(\text{for } \Delta X^2 - \Delta Z^2 \neq 0)$$

or

$$\int_{Y_L(X_i)}^{Y_U(X_i)} \frac{F(X_i,Y) - F(X_i,Y^*)}{R^2} dY - F(X_i,Y^*) \, F.P. \left[\frac{1}{\Delta Y_U} - \frac{1}{\Delta Y_L} \right] \tag{59}$$

Case ii

In this case, a singularity exists in the X-direction as the integration point approaches the apex of the characteristic cone. Rewriting the singular integral using the definition of the inner integral given by Equation (54);

$$I_s = \int_{X_L}^{X_U} \frac{\exp\{-ik M_0 \Delta X\} G(X)}{\Delta X} dX \tag{60}$$

Let X^* be the last X-coordinate in the Gaussian integration then the finite part of this integral is

$$I_s = \int_{X_L}^{X_U} \frac{[\exp\{ikM_0\Delta X\} G(X) - \exp\{-ikM_0\Delta X^*\} G(X^*)]}{\Delta X} dX \tag{61}$$

$$+ \exp\{-ikM_0\Delta X^*\} G(X^*) \ln \Delta X_L$$

Thus, all integrals involved have been formulated for numerical computation with a minimum of singular behavior.

DISCUSSION

The first objective of the study, the extension of the integrated potential method of analysis to the three-dimensional flow-field problem formulation, has been illustrated. In this formulation, the varying Mach number-velocity vector is not treated explicitly. Rather, such variations will be considered in a piecewise fashion, from element to element, and in the determination in a sequential manner of the effective domains of influence and dependence of nodal source and field locations.

Some developments in the formulation of the integral equation are discussed resulting in improved handling of singularities on the Mach cone. These aspects of the formulation are however incomplete (See Appendix).

In particular, the integral equations given in Equation 18 are more complex than those encountered in the planar case. They were therefore checked in a simple configuration in preference to tackling the arbitrarily oriented element. Indeed, general element codings were outside the scope of the task and limited aims have been achieved. In particular, a quadrilateral/triangular element was formulated and coded for restricted circumstances only, with the original intention of applying it to a simple wing-body interference problem.

Instead, a rectangular wing of aspect ratio 2 was treated and is compared in Table 1 with Reference 23. Agreement is limited and improvement is desirable.

After some investigation the source of inaccuracy (suspected as program coding for some time) was found to be in the formulation and computational treatment of the improper integrals. The present status is discussed in the Appendix.

TABLE 1.

COMPARISON OF GENERALIZED AERODYNAMIC FORCES FOR RECTANGULAR WING OF ASPECT RATIO 2.0 AT M_o = 1.2

Mode 1 - Heave

Mode 2 - Pitch about mid-chord

Method		Present		Reference 23	
Number of Elements on Chord		5		30	
k	G.F.	Re	Im	Re	Im
0	Q_{11}	3.31		3.75	
	Q_{22}	-0.5		-0.38	
0.3	Q_{11}	0.0644	0.938	0.188	1.009
	Q_{12}	3.176	0.027	3.369	-0.499
	Q_{21}	-0.043	-0.147	-0.0045	-0.130
	Q_{22}	-0.4685	0.273	-0.4114	0.164
0.6	Q_{11}	0.068	1.730	0.348	1.640
	Q_{12}	3.057	0.3034	2.838	-0.294
	Q_{21}	-0.166	-0.107	-0.2424	-0.2860
	Q_{22}	-0.3307	-0.503	-0.379	0.450

APPENDIX

This section discusses alleviation or elimination of some of the strong singular integrals encountered in the downwash functions (Equation 15). This requires proper ordering of integrations and differentiations.

Consider the downwash integral given by Equation (15)

$$\frac{\partial \phi}{\partial n_o} = \frac{1}{2\pi \ell_r} \int_{X_L}^{X_U} \int_{Y_L}^{Y_U} \exp\{-ik M_o \Delta X\} \cdot \left[\left\{ \frac{\partial}{\partial \nu} \left(\frac{\cos kR}{R} \right) + ik M_o \ell \frac{\cos kR}{R} \right\} \phi(X) - \left\{ \frac{\cos kR}{R} \right\} \frac{\partial \phi}{\partial \nu} \right] dX\, dY \tag{A1}$$

For flat elements (triangular or quadrilateral) the normal and co-normal derivatives can be expressed in terms of local normal and co-normal derivatives, i.e.,

$$\frac{\partial}{\partial \nu'} = -\ell \frac{\partial}{\partial X} + n \frac{\partial}{\partial Z'} \tag{A2}$$

and

$$\frac{\partial}{\partial n_o'} = +\ell_o \frac{\partial}{\partial X_o} + n_o \frac{\partial}{\partial Z_o'} \tag{A3}$$

using Y and Z component velocities expressed in terms of the local Z' component (See Figure A1).

Using the Bessel series expansion for $(\cos kR)/R$ (See Equation 24) the expression in Equation (A1) may be written as

$$\frac{\partial \phi}{\partial n_o'} = \frac{1}{2\pi \ell_r} \frac{\partial}{\partial n_o'} \int_{X_L}^{X_U} \int_{Y_L'}^{Y_U'} \exp\{-ik M_o \Delta X\} \cdot \left[\left\{ -\ell \frac{\partial}{\partial X} \left(\frac{\partial \psi}{\partial Y'} \right) + n' \frac{\partial}{\partial Z'} \left(\frac{\partial \psi}{\partial Y'} \right) + ik M_o \ell \frac{\partial \psi}{\partial Y'} \right\} \phi(X) - \frac{\partial \psi}{\partial Y'} \frac{\partial \phi}{\partial \nu'} \right] dX\, dY' \tag{A4}$$

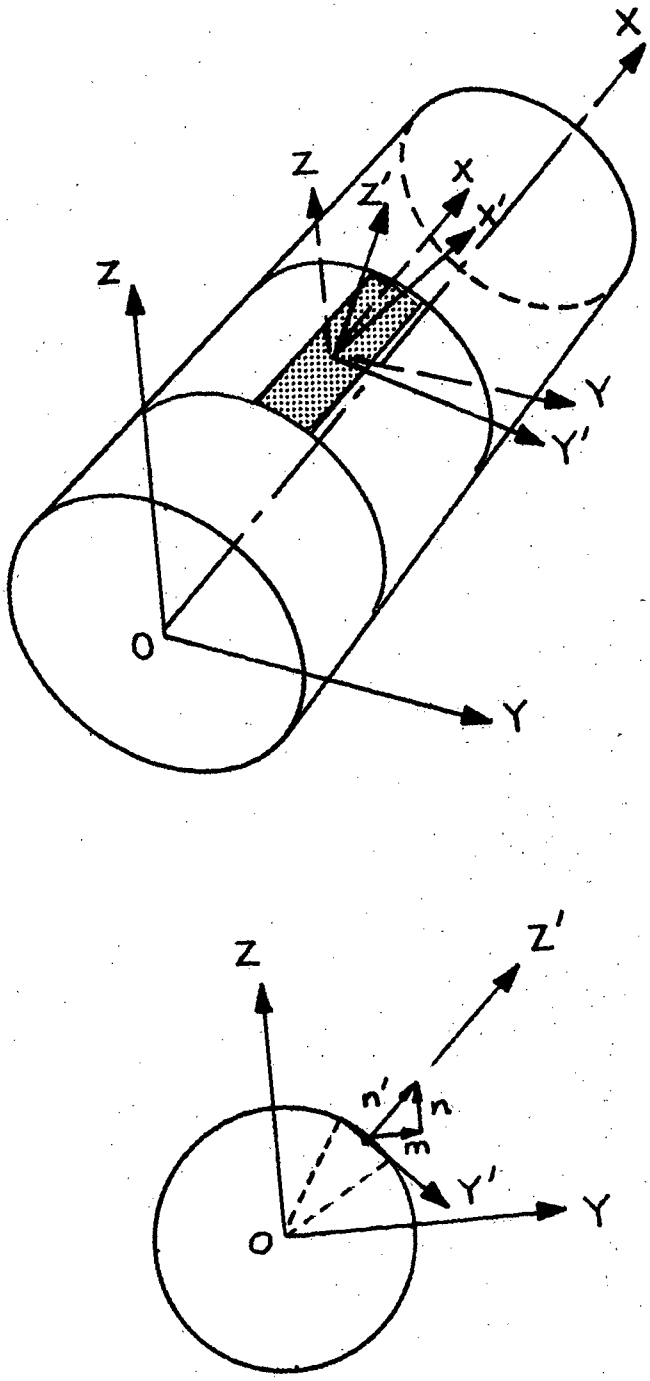

X,Y,Z are the system coordinates

X',Y',Z' are element local coordinates with Z' normal to the plane of the element

FIGURE A1 Local Coordinates and Components of Direction Cosines of a Typical Element

The last two terms can be integrated with respect to Y' in terms of ψ at the upper and lower limits of $Y'(X)$. Should the limits be on the Mach line, the $\mathrm{Sin}^{-1}(\beta/\mu)$ term becomes $\pm \pi/2$ and $\psi \Rightarrow \pm\frac{\pi}{2} J_0(k\mu)$, the derivatives of which exist.

The singular nature of the downwash integral stems from the first two terms i.e., the integrals of the form

$$I_1 = \frac{\partial}{\partial n_0'} \iint \exp\{-ikM_0\Delta X\} \frac{\partial}{\partial X}\left(\frac{\partial \psi}{\partial Y'}\right) \phi(X,Y')\, dX\, dY' \tag{A5}$$

and

$$I_2 = \frac{\partial}{\partial n_0'} \iint \exp\{-ikM_0\Delta X\} \frac{\partial}{\partial Z'}\left(\frac{\partial \psi}{\partial Y'}\right) \phi(X,Y')\, dX\, dY' \tag{A6}$$

Handling of these two integrals will be typified in this section by simple examples. For the sake of simplicity let $\ell = 0$, (representing a planar wing case). Then the downwash integral is represented by

$$w = \frac{1}{2\pi \ell_r} \frac{\partial}{\partial Z_0'} \int_{X_L}^{X_U} \int_{Y_L'(X)}^{Y_U'(X)} \exp\{-ikM_0\Delta X\} \frac{\partial}{\partial Z'}\left(\frac{\partial \psi}{\partial Y'}\right) \phi(X,Y')\, dX\, dY' \tag{A7}$$

Since $Y_U'(X)$ and $Y_L'(X)$ are independent of Z', integration with respect to Y' results in

$$w = \frac{1}{2\pi \ell_r} \frac{\partial}{\partial Z_0'} \int_{X_L}^{X_U} \exp(-ikM_0\Delta X) \frac{\partial}{\partial Z'}\left[\psi \phi(X,Y')\Big|_{Y_L'}^{Y_U'} - \frac{\partial \phi}{\partial Y'} \int_{Y_L'}^{Y_U'} \psi\, dY'\right] dX \tag{A8}$$

(since, in a triangular element, ϕ is linear in X, Y'.)

At the upper and/or lower limits of Y' on the Mach line, the ψ and $\int\psi$ terms are purely functions of $J_0(k\mu)$, the derivatives of which exist. Hence the normal derivatives $\frac{\partial}{\partial n_0'}$ or $\frac{\partial}{\partial z_0'}$ can be performed under the integral sign.

For illustrative purpose let $\phi(X,Y')$ be constant within a triangle. Then Equation (A8) may be written as

$$w = \frac{\phi}{2\pi\ell_r}\frac{\partial}{\partial z_0'}\int_{X_L}^{X_U}\exp\{-ikM_0\Delta X\}\frac{\partial}{\partial z'}\left[\psi(X,Y_U')-\psi(X,Y_L')\right]dX \qquad (A9)$$

where

$$\psi(X,Y_U') = \psi_0+\sum\psi_{2r} \quad \text{for the sides of a triangle not on Mach line.}$$

$$= \pm\frac{\pi}{2}J_0(k\mu) \quad \text{for a side on the Mach line, in which}$$

$$\psi_0 = J_0(k\mu)\sin^{-1}(\gamma/\mu)$$

$$\psi_{2r} = \frac{(-1)^r}{r}J_{2r}(k\mu)\sin\left(2r\sin^{-1}(\gamma/\mu)\right)$$

For a diamond element formed by two triangles (Fig. A2), the contribution from lines CB and C'B is

$$w_B = \frac{\phi_2}{2\ell_r}\lim_{z_0\to z}\int_{X_C}^{X_B}\exp\{-ikM_0\Delta X\}\frac{\partial}{\partial z_0}\cdot\frac{\partial}{\partial z}\left(J_0(k\mu)\right)dX$$

$$= -\frac{k^2\phi_2}{2\ell_r}\int_{X_C}^{X_B}\frac{J_1(k\mu^*)}{k\mu^*}\,dX \qquad (A10)$$

where $\mu^* = X_0 - X$

Note the regularity of the function, $\lim_{\mu\to 0}\frac{J_1(k\mu)}{k\mu} = 1$

which normally would have been singular. For the steady state case ($k=0$) the contribution to the downwash with constant ϕ in element 2 is zero.

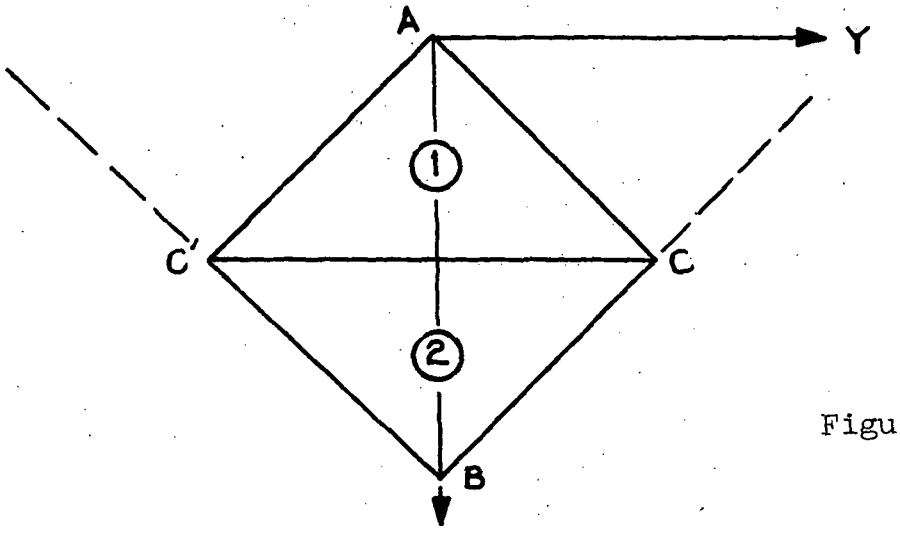

Figure A2

The contribution from the triangle (1) can be obtained by differentiation of the ψ_o and ψ_{2r} functions with respect to z and z_o and taking the limits as $z_o \to z$. Since this is a non-singular element, no elaboration is necessary.

A similar treatment can be applied to elements inclined to the flow direction (i.e., with $\ell \neq 0$).

This illustrates how the strong singular integrals appearing in Equations (12) and (15) can be reformulated so that errors are minimized in the numerical stage.

REFERENCES

1. Appa, K., and Smith, G.C.C., Further Developments in Consistent Unsteady Supersonic Aerodynamic Coefficients. AIAA Journal of Aircraft, Vol. 9, No. 2, Feb 1972.

2. Appa, K., and Smith, G.C.C. Development and Application of Supersonic Unsteady Consistent Aerodynamics for Interfering Parallel Wings. NASA CR-2168, August 1972.

3. Zartarian, G., and Hsu, P.T., Theoretical Studies on the Prediction of Unsteady Supersonic Airloads on Elastic Wings, Parts I & II. WADC Tech Rept. 56-97, 1955.

4. Ashley, H., Supersonic Air Loads on Interfering Lifting Surfaces by Aerodynamic Influence Coefficient Theory. The Boeing Co Rept. No. D2-22067, November 1962.

5. Moore, M.T., and Andrew, L.V., Unsteady Aerodynamics for Advanced Configurations, Parts I to IV. FDL-TDR-64 152, 1965.

6. Donato, V.W., and Huhn, C.R.; Supersonic Unsteady Aerodynamics for Wings With Trailing Edge Control Surfaces and Folded Tips. AFFDL-TR-68-30, August 1968.

7. Stark, V.J.E., Calculation of Aerodynamic Forces on Two Oscillating Finite Wings at Low Supersonic Mach Numbers. SAAB TN53, Sweden 1964.

8. Rubbert, P.E. and Landahl, M.T., Solution of the Transonic Airfoil Problem Through Parametric Differentiations. AIAA Journal, Vol. 5, March 1967.

9. Davidenko, D.F., About the Approximated Solution of A System of Nonlinear Equations. (In Russian) Ukrainian Math. Journal Vol. 5, No. 2, 1953.

10. Kacprzynski, J.J., Ashley, H. and Sankaranarayanan, R., On The Calculation of Unsteady Nonlinear Three-Dimensional Supersonic Flow Past Wings, Trans. ASME Dec. 1968.

11. Ashley, H., Machine Computation of Aerodynamic Loads in Linear and Nonlinear Situations, Proceedings of the 9th Indian Congress of Applied Mechanics, Kanpur, India, 1964 (Also M.I.T. Fluid Dynamics Research Lab. Report 66-5).

REFERENCES (CONT).

12. Smith, A.M.O., Recent Progress in the Calculation of Potential Flows, Douglas Paper 5022, August 1968.

13. Jones, W.P., Supersonic Theory for Oscillating Wings of Any Planform. A.R.C. R&M 2655, June 1948.

14. Woodward, F.A., Analysis and Design of Wing-Body Combinations at Subsonic and Supersonic Speeds. AIAA Journal of Aircraft, Vol. 5, No. 6,1968.

15. Cunningham, H.J., Improved Numerical Procedure for Harmonically Deforming Lifting Surfaces From The Supersonic Kernel Function Method, AIAA Journal, Vol. 4 No. 11, November 1966.

16. Garrick, I.E., and Rubinow, S.I., Theoretical Study of Air Forces on An Oscillating or Steady Thin Wing in a Supersonic Main Stream. NACA Report 827, 1947.

17. Appa, K., Kinematically Consistent Unsteady Aerodynamic Coefficients in Supersonic Flow. International J. for Numerical Methods in Engineering, Vol. 2, pp 495-507, October 1970. (Also National Aeronautical Laboratories NAL TN-9, India, March 1968).

18. Woodcock, D.L. and Lawrence, A.J., Flutter Research in the United Kingdom. 1969-71. R.A.E. Tech Memo. Structures 813, September 1971.

19. Heaslet, M.A., Lomax, H. and Jones, A.L., Volterra's Solution of the Wave Equation as Applied to Three Dimensional Supersonic Airfoil Problems. NACA Report 889, 1947.

20. Allen, D.J. and Sadler, D.S., Oscillatory Aerodynamic Forces in Linearized Supersonic Flow for Arbitrary Frequencies, Planforms, and Mach Numbers. A.R.C. R&M, No. 3415, January 1963.

21. Woodcock, D.L. and York, E.J., A Supersonic Box Collocation Method for the Calculation of Unsteady Airforces of Tandem Surfaces. Symposium on Unsteady Aerodynamics for Aeroelastic Analyses of Interfering Surfaces, Part I; AGARD-CP-80-71.

22. Watson, G.N., Theory of Bessel Functions. 2nd Edition Cambridge University Press 1948.

23. Laschka, B.; et al, Generalized Aerodynamic Forces for Some Wing Planforms According to the Linearized Three-Dimensional Lifting Surface Theory in Subsonic and Supersonic Flow. VFW No. M-75/66, Dec. 1966. AGARD Structures and Materials Meeting. Ottawa, Sept. 1967.